Journal of Sound and Vibration (2001) **243**(4), 699–719
doi:10.1006/jsvi.2000.3431, available online at http://www.idealibrary.com on IDEAL®

ON THE ACOUSTO-ELASTIC BEHAVIOUR OF DOUBLE-WALL PANELS WITH A VISCOTHERMAL AIR LAYER

T. G. H. Basten, P. J. M. van der Hoogt, R. M. E. J. Spiering and H. Tijdeman

Department of Mechanical Engineering, University of Twente, P.O. Box 217, 7500 *AE Enschede, The Netherlands. E-mail: t.g.h.basten@wb.utwente.nl*

(*Received* 8 *May* 2000, *and in final form* 29 *September* 2000)

In this paper, an analytical two-dimensional model is presented for the acousto-elastic behaviour of double-wall panels with a thin viscothermal air layer. The model for the air is based on the low reduced frequency solution as introduced by Beltman (1998 *Ph.D. Thesis, University of Twente*; 1999 *Journal of Sound and Vibration* **227**, (Part I), 555–586; **227** (Part II), 587–609; Beltman *et al.*, 1997 *Journal of Sound and Vibration* **206**, 217–241; 1998 *Journal of Sound and Vibration* **216**, 159–185) [1–5] and includes, apart from inertia and compressibility, the effects of viscosity and thermal conductivity. With the analytical model eigenfrequencies were determined and response and transmission calculations were performed. It is shown that high damping coefficients for double-wall panels can be obtained by using the viscous characteristics of the fluid layer. The model makes it possible to conduct parameter analyses very easily and efficiently, which is important for design studies. Furthermore, the model gives exact results for both the vibrational behaviour and the sound transmission characteristics of double-wall panels which can be used to validate numerical codes.

1. INTRODUCTION

Double-wall structures consisting of two flexible plates separated by a thin air layer as shown in Figure 1 are often used to minimize to the sound transmission from one room to another or from noisy machinery to the environment. Beranek and Work [6] were among the first to set up a model for the sound transmission through unbounded double walls with an inviscid fluid in between. A similar model was used by London [7]. Mulholland *et al.* [8] included sound absorbing material. Trochidis [9] and Trochidis and Kalaroutis [10] modelled the dissipative behaviour of double-wall panels by incorporating the viscosity of the medium. They also took into account the flexibility of the walls. However, they modelled only one-way coupling, i.e., they used the vibrational behaviour of the plate as a boundary condition for the fluid. Möser [11] extended their model with compressibility effects. Fully coupled models with viscothermal effects were developed by Fox and Whitton [12], Önsay [13] and Beltman [1]. For double walls with large gaps, a model which is based on the uncoupled modal behaviour is often used, e.g., Desmet and Sas [14]. For high frequencies statistical models can be applied, e.g., reference [15]. In the present paper, the fully coupled model with viscothermal effects developed by Beltman will be applied to model double-wall panels with a thin viscothermal air layer. This model is very efficient and is complete, i.e., it includes all relevant effects. Furthermore, it is suitable for parameter studies. Besides the vibro-acoustic behaviour of the panel, the sound radiation

0022-460X/01/240699 + 21 $35.00/0

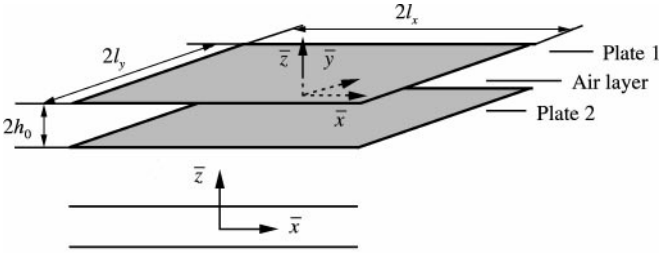

Figure 1. Double-wall panel with thin air layer.

characteristics of the structure will also be considered. First, the coupled acousto-elastic model will be presented. For a given configuration results of modal and harmonic response calculations will be presented. In the latter part, sound transmission characteristics of the double-wall panel will be discussed.

2. MODEL FOR THE DOUBLE-WALL PANEL

For the dynamical behaviour of the double-wall structure a fully coupled formulation is used based on the low reduced frequency model for the air layer between the plates and the Kirchhoff plate equation for the structural behaviour of the plates [6]. There is no coupling between the external air and the plates, because its influence on the dynamical behaviour of the panel is very low compared with the influence of the air layer. In this section the model for a finite double-wall panel will be presented. In the subsequent sections, numerical results for a two-dimensional configuration without variations in the $\bar{y}$ direction will be considered.

2.1. LOW REDUCED FREQUENCY MODEL

In Figure 1, two flexible plates, 1 and 2, with identical dimensions $2l_x$ and $2l_y$ but different thicknesses t_1 and t_2 are located parallel to each other. They perform small harmonic oscillations in $\bar{z}$ direction with an angular frequency ω around their equilibrium positions. The distance between the plates is given by $\bar{h}(\bar{x}, \bar{y}, t)$ and $2h_0$ is the mean thickness of the air layer. Beltman *et al.* [2] derived a low reduced frequency model for the viscothermal wave propagation in the air layer. This model includes the effects of inertia, compressibility, viscosity and thermal conductivity of the air. The model is derived from the Navier–Stokes equation, the equation of continuity, the equation of state for an ideal gas and the energy equation. The basic assumptions are that the perturbations are small and harmonic, there is no mean flow and no internal heat generation, the fluid is homogeneous and the oscillating flow is laminar. Furthermore, it is assumed that the thickness of the air layer is much smaller than the acoustic wavelength. Therefore, the pressure distribution can be assumed to be constant across the air layer. The perturbations are written in non-dimensional form by using undisturbed conditions.[†] The velocity of the air in the layer is made dimensionless with the speed of sound c_0. Note that in the low reduced frequency model the velocity, density and temperature perturbations, in contrast with the pressure, vary across the layer thickness:

[†]A list of symbols is given in Appendix B.

- Distance between the flexible plates:

$$\bar{h}(x, y, t) = h_0[2 + [h_1(x, y) - h_2(x, y)]\,\mathrm{e}^{\mathrm{i}\omega t}], \tag{1}$$

- Pressure in the air layer:

$$\bar{p}(x, y, t) = p_0[1 + p(x, y)\mathrm{e}^{\mathrm{i}\omega t}], \tag{2}$$

with $p_0 = c_0^2\rho_0/\gamma$,

- Density in the air layer:

$$\bar{\rho}(x, y, z, t) = \rho_0[1 + \rho(x, y, z)\mathrm{e}^{\mathrm{i}\omega t}], \tag{3}$$

- Temperature in the air layer:

$$\bar{T}(x, y, z, t) = T_0[1 + T(x, y, z)\mathrm{e}^{\mathrm{i}\omega t}], \tag{4}$$

- Velocity in the air layer:

$$\bar{\mathbf{v}}(x, y, z, t) = c_0\mathbf{v}(x, y, z)\mathrm{e}^{\mathrm{i}\omega t}. \tag{5}$$

The dimensionless co-ordinates are given by $x = \omega\bar{x}/c_0$, $y = \omega\bar{y}/c_0$ and $z = \bar{z}/h_0$. When the following dimensionless numbers are introduced, $k_{px} = \omega l_x/c_0$ and $k_{py} = \omega l_y/c_0$ the dimensionless co-ordinates vary as $-k_{px} \leqslant x \leqslant k_{px}$, $-k_{py} \leqslant y \leqslant k_{py}$ and $-1 \leqslant z \leqslant 1$.

The dimensionless perturbations are substituted in the basic equations and the higher order terms are neglected. The resulting equations for the perturbations can be written in a linear non-dimensional form [1]. The linearized equation for the pressure perturbation of the fluid in the air layer is

$$\boldsymbol{\nabla}^2 p - \Gamma(s)^2 p = n(s\sigma)\Gamma(s)^2\tfrac{1}{2}[h_1 - h_2], \tag{6}$$

where the non-dimensional operator $\boldsymbol{\nabla}^2$ is given by

$$\boldsymbol{\nabla}^2 = \frac{\partial^2}{\partial x^2} + \frac{\partial^2}{\partial y^2}. \tag{7}$$

In the low reduced frequency model several independent dimensionless parameters can be distinguished:

shear wave number: $s = h_0\sqrt{\dfrac{\rho_0\omega}{\mu}}$,

reduced frequency: $k = \dfrac{\omega h_0}{c_0}$,

square root of the Prandtl number: $\sigma = \sqrt{\dfrac{\mu C_p}{\lambda}}$,

ratio of specific heats: $\gamma = \dfrac{C_p}{C_v}$,

where μ is the dynamic viscosity, λ is the thermal conductivity and C_p and C_v are the specific heats at constant pressure and at constant volume respectively. The propagation of pressure perturbations is determined by the propagation coefficient $\Gamma(s)$. This coefficient is a function of the shear wave number and thus also of the frequency:

$$\Gamma(s) = \sqrt{\frac{\gamma}{n(s\sigma)B(s)}}, \tag{8}$$

$$B(s) = \frac{\tanh(s\sqrt{\mathrm{i}})}{s\sqrt{\mathrm{i}}} - 1, \tag{9}$$

$$n(s\sigma) = \left[1 + \left(\frac{\gamma - 1}{\gamma}\right) B(s\sigma)\right]^{-1}. \tag{10}$$

The wave propagation in the air layer is affected by thermal and viscous effects. The function $B(s)$ includes the viscous effects, whereas $n(s\sigma)$, which can be interpreted as a polytropic coefficient, accounts for the thermal effects. Note that the product $s\sigma$ in equation (10) does not depend on the viscosity μ so only thermal effects are involved. The polytropic coefficient relates the pressure to the density in a polytropic relation:

$$\frac{\bar{p}}{\bar{\rho}^{n(s\sigma)}} = \text{constant}. \tag{11}$$

The right-hand side of equation (6) takes into account the motion of the plates. The low reduced frequency model can be used when the following conditions are fulfilled: $k \ll 1$ and $k/s \ll 1$, which means that, among others, the thickness of the air layer is much smaller than the acoustic wavelength. Only in extreme situations these conditions are not fulfilled as shown by Beltman [1]. In the present study the conditions are satisfied.

2.2. KIRCHHOFF PLATE EQUATION

To describe the motion of both thin plates, subjected to the pressure field in the air layer, the so-called Kirchhoff equation is applied. The Kirchhoff equation is valid for the vibrational behaviour of thin isotropic plates with constant thickness. Only bending stresses are taken into account and normals to the midsurface of the undeformed plate remain straight and normal to the midplane during deformation. Rotary inertia and shear deformations are neglected. The equations of motion read:

$$\nabla^4 h_1 - \frac{\Omega_1^2}{k_{px}^4} h_1 = \frac{\Omega_1^2 \varepsilon_1}{\gamma k_{px}^4 k^2} p, \tag{12}$$

$$\nabla^4 h_2 - \frac{\Omega_2^2}{k_{px}^4} h_2 = -\frac{\Omega_2^2 \varepsilon_2}{\gamma k_{px}^4 k^2} p, \tag{13}$$

where the non-dimensional operator ∇^4 is

$$\nabla^4 = \frac{\partial^4}{\partial x^4} + 2\frac{\partial^4}{\partial x^2 \partial y^2} + \frac{\partial^4}{\partial y^4} \tag{14}$$

and the dimensionless frequency Ω_j is

$$\Omega_j = \omega \sqrt{\frac{l_x^4 \rho_{pj} t_j}{D_j}}. \tag{15}$$

ρ_{pj} is the density of the plate material and D_j the bending stiffness of plate j (j equals 1 or 2). D_j is given by

$$D_j = \frac{E_j t_j^3}{12(1 - v_j^2)}, \tag{16}$$

where E_j and v_j are Young's modulus and Poisson's ratio respectively. The dimensionless constant $\varepsilon_j = \rho_0 h_0 / \rho_{pj} t_j$ is a measure for the ratio of mass per unit area between the air layer and plate j. The right-hand sides of equations (12) and (13) represent the influence of the air layer on the dynamical behaviour of the two plates. Note that for $p = 0$ the uncoupled equations of motion for the plates in vacuum are obtained.

2.3. PROBLEM DEFINITION

The models derived in the previous sections lead to a coupled formulation for the double-wall panel. For convenience of the reader the equations governing the problem are summarized:

$$\nabla^2 p - \Gamma(s)^2 p = n(s\sigma)\Gamma(s)^2 \tfrac{1}{2}[h_1 - h_2], \tag{17}$$

$$\nabla^4 h_1 - \frac{\Omega_1^2}{k_{px}^4} h_1 = \frac{\Omega_1^2 \varepsilon_1}{\gamma k_{px}^4 k^2} p, \tag{18}$$

$$\nabla^4 h_2 - \frac{\Omega_2^2}{k_{px}^4} h_2 = -\frac{\Omega_2^2 \varepsilon_2}{\gamma k_{px}^4 k^2} p. \tag{19}$$

In the remaining of this paper the vibro-acoustic behaviour of a double-wall panel with simply supported aluminium plates separated by a viscothermal air layer will be investigated. The plate is infinite in the y direction and only variations in the x direction will be considered. The following material properties are used:

$$\begin{aligned} \rho_{p1,2} &= 2710 \text{ kg/m}^3, \quad E_{1,2} = 70 \times 10^9 \text{ N/m}^2, \quad v_{1,2} = 0{\cdot}3, \\ \rho_0 &= 1{\cdot}2 \text{ kg/m}^3, \quad c_0 = 340 \text{ m/s}, \quad \mu = 18{\cdot}2 \times 10^{-6} \text{ Pa s}, \\ \lambda &= 25{\cdot}6 \times 10^{-3} \text{ W/m K}, \quad C_p = 1004 \text{ J/kg K}, \quad \gamma = 1{\cdot}4. \end{aligned} \tag{20}$$

Note that the Young's modulus is a real number so no structural damping is involved. The only damping in the double-wall panel is introduced via the air layer.

3. EIGENFREQUENCIES

In this section, eigenfrequencies for various thicknesses of the air layer are presented. For reasons of convenience, only simply supported double-wall panels which are infinite in the

y direction and where the air in the layer is free to escape along the edges, are discussed. For the two-dimensional panel the following boundary conditions have to be fulfilled:

- Air layer: open edges: $p = 0$ for $x = \pm k_{px}$.
- Plates 1 and 2: zero deflection: $h_{1,2} = 0$ and zero bending moment: $d^2h_{1,2}/dx^2 = 0$ for $x = \pm k_{px}$.

From the differential equations and the boundary conditions, the eigenfrequencies and mode shapes of the coupled system can be derived. Equations (17)–(19) lead to a sixth order characteristic equation in ω. An iterative root finding procedure is used to obtain the, in general complex, eigenfrequencies and their corresponding eigenmodes (see also Appendix A). The viscous damping coefficient corresponding with angular eigenfrequency ω_r is calculated from

$$\zeta_r = \frac{\mathrm{Im}(\omega_r)}{|\omega_r|} \times 100\%, \tag{21}$$

where r is the mode number. For the present configuration, the rth eigenfunction describing the motion of the first panel is of the form:

$$h_1(x) = A_r \sin\left(\frac{r\pi}{2}\left(\frac{x}{k_{px}} + 1\right)\right). \tag{22}$$

The eigenfunctions describing the motion of the second panel and the pressure in the air layer depend on the situation considered. Two different situations are distinguished:

- Identical plates (equal thickness).
- Non-identical plates (different thickness).

3.1. IDENTICAL PLATES

When both plates have the same thickness and are vibrating in phase, the eigenfunction of the second plate is equal to the eigenfunction of the first plate:

$$h_2(x) = A_r \sin\left(\frac{r\pi}{2}\left(\frac{x}{k_{px}} + 1\right)\right). \tag{23}$$

Because there is no relative displacement between the panels, the resulting pressure perturbation is zero,

$$p(x) = 0. \tag{24}$$

For this situation, the eigenfrequencies of the system remain the same as for the panels in vacuum, given by

$$f_{vac,r,j} = \frac{1}{2\pi}\left(\frac{r\pi}{2}\right)^2 \sqrt{\frac{D_j}{l_x^4 \rho_{pj} t_j}}. \tag{25}$$

Obviously, there is no influence of the air layer on the dynamical behaviour of the panels; the eigenfrequencies are independent of the thickness of the air layer and no damping is

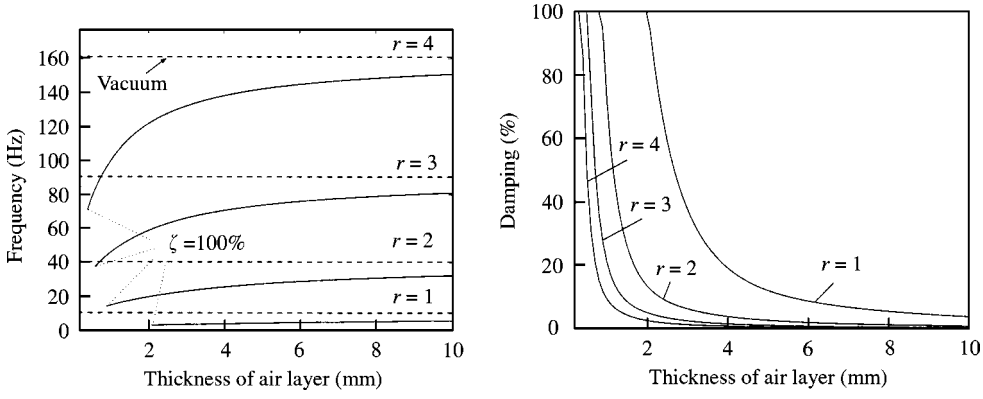

Figure 2. Eigenfrequencies and damping coefficients of the first four out-of-phase modes of the identical double-panel system.

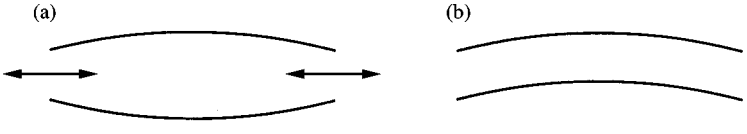

Figure 3. (a) Pumping effect for a double-wall panel with plates vibrating out of phase. (b) For the in-phase vibration the amplitudes are equal so there is no pumping effect.

created. In reality, however, there will be a very small added mass effect of the air layer on the vibration of the plates. Because in the low reduced frequency model the inertia forces in the z direction are neglected, the model does not predict any influences of the air layer in this situation.

When the plates are vibrating out of phase, the eigenfunctions for the pressure and the second plate, respectively, are

$$p(x) = A_r \frac{k^2\gamma}{\Omega_1^2 \varepsilon_1}\left[\left(\frac{r\pi}{2}\right)^2 - \Omega_1^2\right] \sin\left(\frac{r\pi}{2}\left(\frac{x}{k_{px}} + 1\right)\right), \tag{26}$$

$$h_2(x) = -A_r \sin\left(\frac{r\pi}{2}\left(\frac{x}{k_{px}} + 1\right)\right). \tag{27}$$

Note that for identical panels $\Omega_1 = \Omega_2$ and $\varepsilon_1 = \varepsilon_2$. In Figure 2, the eigenfrequencies and damping values of the first four out-of-phase eigenmodes are given as a function of the thickness of the air layer for the situation with $t_1 = t_2 = 1{\cdot}0$ mm. The value for l_x is 0·245 m. For this situation the first four in-vacuum frequencies are 10·1, 40·2, 90·6 and 161·0 Hz respectively. The influence of the air layer on the eigenfrequencies of the plates increases for decreasing thickness of the air layer. The eigenfrequencies in the situation with air layer are lower than the frequencies in vacuum, due to the added mass effect caused by pumping of air in the air layer (see Figure 3). The damping increases for decreasing thickness of the air layer. For a large thickness of the air layer, the eigenfrequencies of the double-panel system approach the eigenfrequencies in vacuum. In the calculations the thickness of the air layer is decreased until a critical damping situation ($\zeta = 100\%$) is reached. The critical damping situation is chosen because for higher damping values a very strong coupling between the

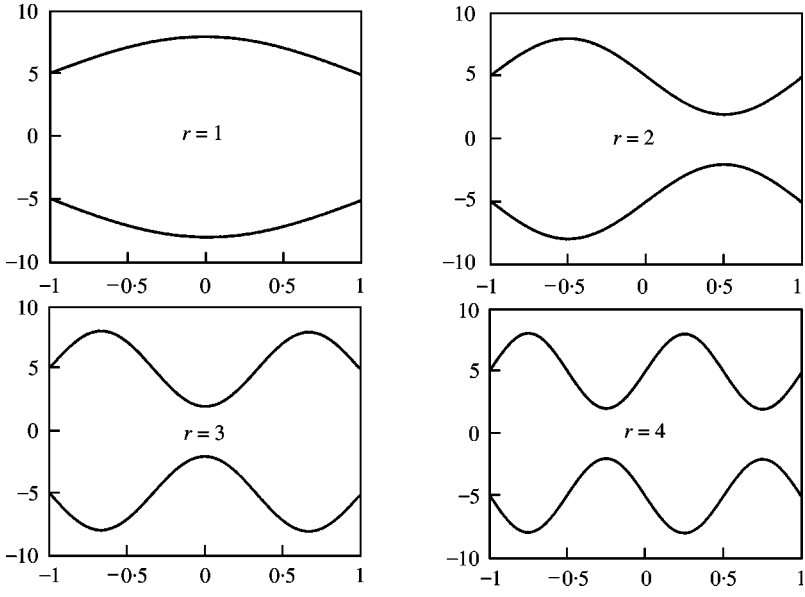

Figure 4. First four out-of-phase mode shapes of the identical panel system, $2h_0 = 10$ mm.

plates exists. This situation has to be avoided so that pumping of air is preserved. It will be clear that for the vacuum situation the damping equals zero. The mode shapes for $2h_0 = 10$ mm are given in Figure 4.

3.2. NON-IDENTICAL PLATES

The eigenfunctions for the pressure and the motion of the second plate for two non-identical plates vibrating in phase, are given by

$$p(x) = A_r \frac{k^2\gamma}{\Omega_1^2 \varepsilon_1}\left[\left(\frac{r\pi}{2}\right)^4 - \Omega_1^2\right] \sin\left(\frac{r\pi}{2}\left(\frac{x}{k_{px}} + 1\right)\right), \tag{28}$$

$$h_2(x) = -A_r \frac{\Omega_2^2 \varepsilon_2}{\Omega_1^2 \varepsilon_1} \frac{[(r\pi/2)^4 - \Omega_1^2]}{[(r\pi/2)^4 - \Omega_2^2]} \sin\left(\frac{r\pi}{2}\left(\frac{x}{k_{px}} + 1\right)\right). \tag{29}$$

The eigenfrequencies and damping values as a function of the thickness of the air layer of the first four modes for the situation with $t_1 = 1$ mm and $t_2 = 2$ mm are given in Figure 5, the value for l_x is again 0·245 m. The eigenfrequencies of the thickest plate in vacuum are 20·1, 80·5, 181·1 and 322·0 Hz. Therefore, it can be seen that the coupled eigenfrequencies are dominated by the thickest plate. The coupled eigenfrequencies are lower than in vacuum, because of two reasons. The first reason is that there is a small added mass effect because of the air in the gap. Both plates do not move with the same amplitude, so there is a net pumping effect in the air layer, as sketched in Figure 6. However, the effect is considerably less than for the out-of-phase situation as can be seen from the damping curve in Figure 5. The second and main reason for the eigenfrequencies of the double-wall panel to decrease is that the two plates for small air layers are coupled in such a way that they

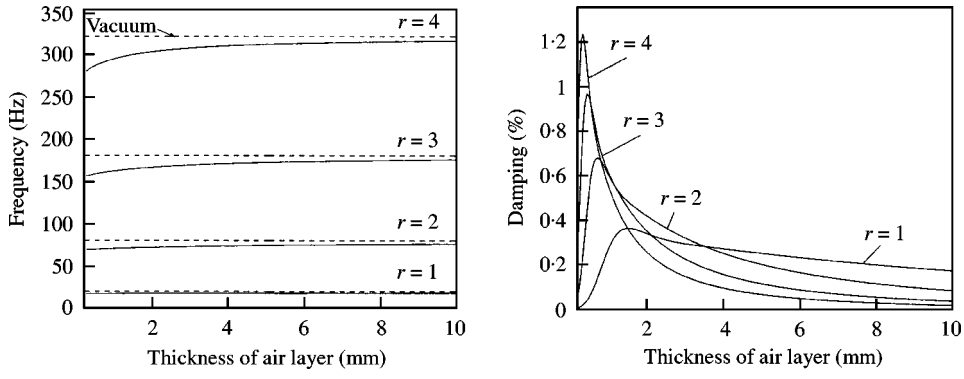

Figure 5 . Eigenfrequencies and damping coefficients of the first four in-phase modes of the double-wall panel with non-identical plates.

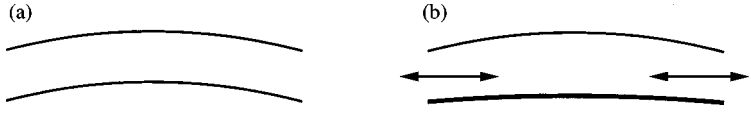

Figure 6. Pumping effect for a double-wall panel with plates vibrating in phase. (a) For identical plates the amplitudes are equal so there is no pumping effect. (b) For non-identical plates there is a small pumping effect due to a difference in amplitude.

vibrate as one panel with a stiffness equal and mass equal to

$$D_{total} = D_1 + D_2 = \left(\left(\frac{t_1}{t_2}\right)^3 + 1\right) D_2 = \frac{9}{8} D_2,$$
$$m_{total} = m_1 + m_2 = \left(\frac{t_1}{t_2} + 1\right) m_2 = \frac{3}{2} m_2. \tag{30}$$

From the expression for the vacuum frequencies, equation (25), it follows that the resulting eigenfrequencies are $\sqrt{4/3}$ times lower than the vacuum frequencies of plate 2. For small air layers there is hardly any pumping effect, so the damping coefficients become very small. The eigenfrequencies and damping values as a function of the thickness of the air layer for two plates vibrating out of phase for the situation with $t_1 = 1$ mm and $t_2 = 2$ mm are given in Figure 7. From the figures it follows that the out-of-phase modes are dominated by the thinnest plate. This is the reason why Figures 2 and 7 show a large resemblance.

The results so far demonstrate that high damping levels can be obtained for double-wall panels with narrow air layers between them.

4. HARMONIC RESPONSE

In this section the response of the double-wall panel to a harmonic excitation is considered. The response behaviour forms the basis for the transmission of sound as will be discussed in the next section.

Suppose that the first plate is subjected to a harmonic external pressure field $F(x, t) = f(x)e^{i\omega t}$ (see Figure 8). Equation (18) changes into

$$\frac{d^4 h_1}{dx^4} - \frac{\Omega_1^2}{k_{px}^4} h_1 = \frac{\Omega_1^2 \varepsilon_1}{\gamma k_{px}^4 k^2} p - f(x). \tag{31}$$

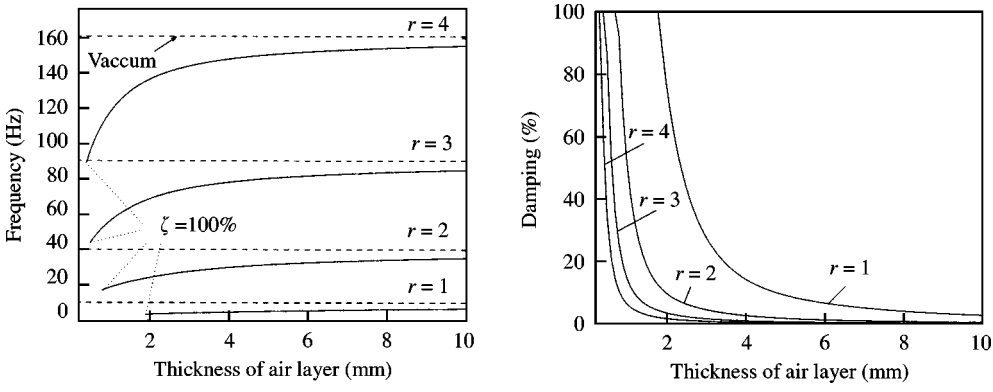

Figure 7. Eigenfrequencies and damping of the first four out-of-phase modes of the non-identical double-panel system.

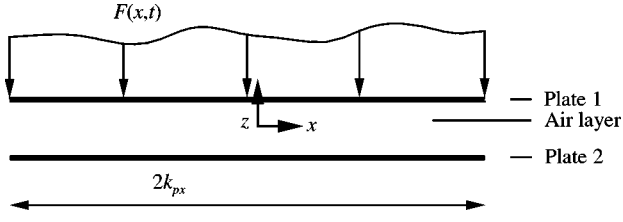

Figure 8. Double-wall panel subjected to an external pressure field.

The responses of plate 1, plate 2, and the air layer are written as linear combinations of eigenmodes:

$$h_1(x) = \sum_{r=1}^{\infty} A_r \sin\left(\frac{r\pi}{2}\left(\frac{x}{k_{px}}+1\right)\right), \tag{32}$$

$$h_2(x) = \sum_{r=1}^{\infty} B_r \sin\left(\frac{r\pi}{2}\left(\frac{x}{k_{px}}+1\right)\right), \tag{33}$$

$$p(x) = \sum_{r=1}^{\infty} C_r \sin\left(\frac{r\pi}{2}\left(\frac{x}{k_{px}}+1\right)\right). \tag{34}$$

Substitution of equations (32)–(34) into the equations of motion ((17), (31) and (19)) yields the participation factors:

$$A_r = \frac{-k_{px}^4 F_r}{\eta_{r,1} + \Omega_1^2 \varepsilon_1 [\Omega_2^2 \varepsilon_2/\eta_{r,2} - k^2 Q_r(s)/k_{px}^2]^{-1}}, \tag{35}$$

$$B_r = \frac{-k_{px}^4 F_r}{\eta_{r,1}[1 - Q_r(s)\, k^2 \eta_{r,2}/k_{px}^2 \Omega_2^2 \varepsilon_2] + \eta_{r,2} \Omega_1^2 \varepsilon_1/\Omega_2^2 \varepsilon_2}, \tag{36}$$

$$C_r = \frac{k_{px}^4 F_r}{\eta_{r,1}[\Omega_2^2 \varepsilon_2 k^2 \gamma \eta_{r,2} - Q_r(s)/k_{px}^2 \gamma] + \Omega_1^2 \varepsilon_1/k^2 \gamma} \tag{37}$$

with

$$\eta_{r,1} = \left(\frac{r\pi}{2}\right)^4 - \Omega_1^2, \quad \eta_{r,2} = \left(\frac{r\pi}{2}\right)^4 - \Omega_2^2, \tag{38}$$

$$\varepsilon_1 = \frac{\rho_0 h_0}{\rho_{p1} t_1}, \quad \varepsilon_2 = \frac{\rho_0 h_0}{\rho_{p2} t_2}, \tag{39}$$

$$F_r = \frac{1}{k_{px}} \int_{-k_{px}}^{k_{px}} f(x) \sin\left(\frac{r\pi}{2}\left(\frac{x}{k_{px}} + 1\right)\right) \mathrm{d}x, \qquad Q_r(s) = -\left[2B(s)\left(\frac{r\pi}{2}\right)^2 + \frac{k_{px}^2 \gamma}{n(s\sigma)}\right]. \tag{40}$$

The dimensionless frequency response function for the second plate becomes

$$H(\omega, x_p) = \frac{h_2(x_p)}{G} = \frac{1}{G} \sum_{r=1}^{\infty} \frac{-F_r k_{px}^4 \sin(r\pi/2(x_p + 1))}{\eta_{r,1}[1 - Q_r(s)\, k^2 \eta_{r,2}/k_{px}^2 \Omega_2^2 \varepsilon_2] + \eta_{r,2} \Omega_1^2 \varepsilon_1 / \Omega_2^2 \varepsilon_2} \tag{41}$$

with

$$G = \int_{-k_{px}}^{k_{px}} |f(x)| \, \mathrm{d}x, \tag{42}$$

and x_p the location on the second plate where the response is calculated. In order to excite both the symmetric and asymmetric modes a pressure field is chosen which consists of a symmetric and an asymmetric part:

$$f(x) = (x/k_{px}) + 1. \tag{43}$$

For this pressure field $G = 2k_{px}$ and $F_r = -4/r\pi(-1)^r$. The response of the identical and non-identical double-wall structures is calculated for the frequency interval 1–180 Hz and a layer thickness which varies from 1 to 50 mm. The results for $x_p = k_{px}/4$ (or $\bar{x} = l_x/4$) are given in Figure 9. This figure shows that the response of a double-wall panel changes drastically with decreasing thickness of the air layer between the plates. As expected, the in-phase frequencies for the identical panel system (which are 10·1, 40·2, 90·6 and 161·0 Hz, respectively), do not depend on the thickness of the air layer. All other eigenfrequencies decrease for decreasing thickness of the air layer and it can be seen from the decrease and widening of the peaks that the damping increases. For relative large thicknesses of the air layer the height of the peaks fluctuates a little. This has no physical meaning but can be attributed to the discretization of the frequency interval. For the non-identical panel system both the in-phase and the out-of-phase frequencies decrease and also in this case the damping increases for decreasing thickness of the air layer.

5. SOUND TRANSMISSION

As a next step, the sound fields which are produced by a vibrating panel will be considered. When the normal velocity distribution of the panel is known, the generated acoustic pressure field on the outside of the two plates can be calculated with the Rayleigh integral for two-dimensional sound radiation. In order to do so, it has to be assumed that the double-wall panel is placed in an infinite baffle (see Figure 10). The pressure at any position x on the plate is found as a summation of contributions of the deflections of each

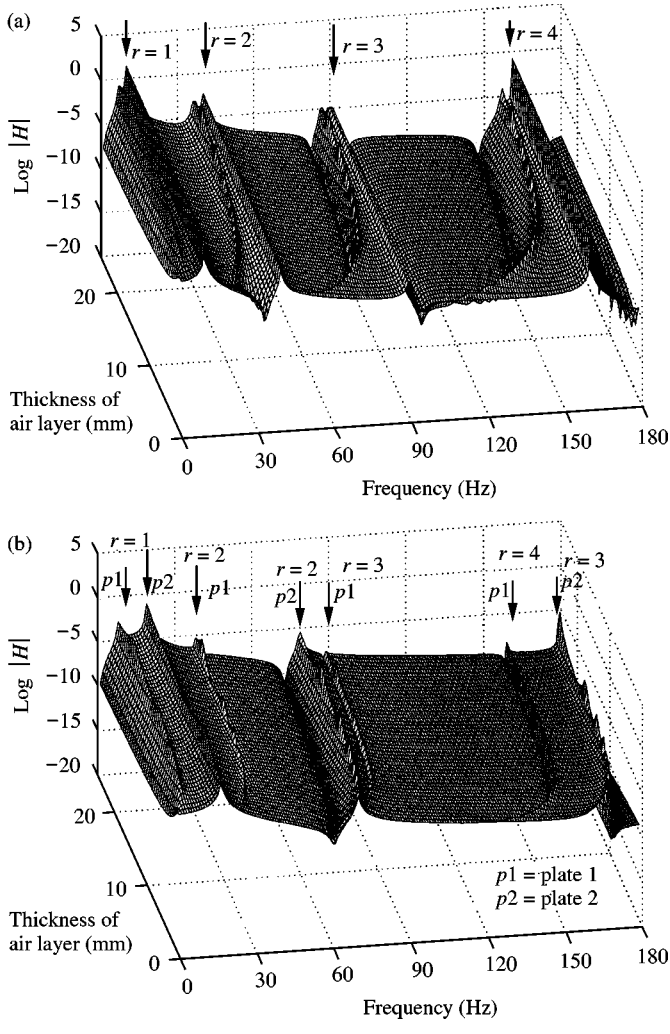

Figure 9. Frequency response function for the identical (a) and non-identical (b) double-wall panel as a function of the thickness of the air layer.

point x' of the plate:

$$p(\omega, x) = \frac{ijk}{2} \int_{-k_{px}}^{k_{px}} h(x') \, \mathrm{H}_0^2(|x - x'|) \, \mathrm{d}x'. \tag{44}$$

H_0^2 is the Hankel function of the second kind, order zero. It is a combination of Bessel functions of the first kind, order zero J_0 and of the second kind, order zero Y_0:

$$\mathrm{H}_0^2 = \mathrm{J}_0 - \mathrm{i}\mathrm{Y}_0 \tag{45}$$

The sound power per unit width radiated by each plate is obtained by integrating the sound intensity over the panel length:

$$\bar{W}_{rad} = \int_{-l_x}^{l_x} \bar{I}_n \, \mathrm{d}\bar{x} = \frac{p_0 h_0 c_0}{2} \int_{-k_{px}}^{k_{px}} \mathrm{Im}[p(x) h(x)^*] \, \mathrm{d}x, \tag{46}$$

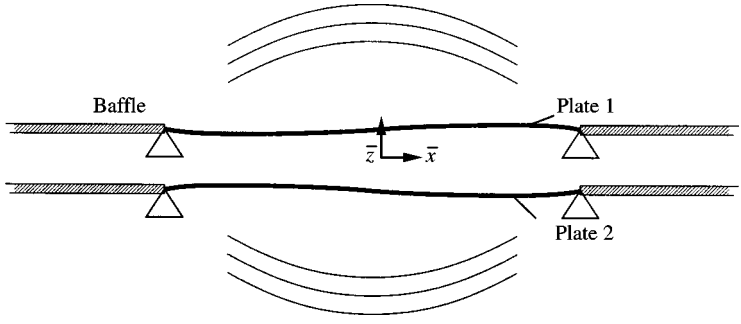

Figure 10. Two-dimensional sound radiation of a double-wall panel in an infinite baffle.

where $\bar{I}_n$ is the time-averaged normal intensity. $p(x)$ and $h(x)^*$ are the complex dimensionless amplitudes of the pressure and complex conjugate of the plate deflection at position x on the plate respectively.

5.1. ENERGY DISSIPATION WITH A PRESSURE FIELD EXCITATION

When the pressure field given in equation (43) is used, the power per unit width which is dissipated by the double-wall panel can be calculated with (note that force and displacement are defined in opposite direction):

$$\bar{W}_d = -\frac{D_1 h_0^2 \omega^4}{2c_0^3} \int_{-k_{px}}^{k_{px}} \mathrm{Im}(f(x)h^*(x))\,\mathrm{d}x. \tag{47}$$

Due to conservation of energy the total power per unit width incident on the panel is $\bar{W}_{in} = \bar{W}_d + \bar{W}_{rad,1} + \bar{W}_{rad,2}$. The energy loss is defined as the fraction of energy put into the system that is dissipated by the air layer,

$$EL = \bar{W}_d / \bar{W}_{in}. \tag{48}$$

The energy loss is a real quantity varying from 0 to 1. For the given pressure field the incident and dissipated power are calculated using trapezoidal numerical integration. The energy loss is calculated for the double-wall panel with identical and non-identical plates. The results, given in Figure 11, make clear that in the given frequency domain the fraction of energy which is dissipated for the non-identical plates is much higher than for the identical plates. As mentioned earlier, for the non-identical plates the pumping effect is much higher than for the identical plates. For the identical plates the energy loss is zero for the in-phase modes while for the non-identical plates there is still some energy loss in the in-phase modes, caused by a relative motion of the two plates.

5.2. POINT EXCITATION

Because in experimental investigations one of the panels is often excited with a shaker [17], the behaviour of a double-wall panel is also investigated for point excitations. A point excitation is put on the first plate, $f(x) = F\delta(x - x_f)$, where δ is the Dirac function and $x_f = k_{px}/2$ (or $\bar{x}_f = l_x/2$) is the location of the force on plate 1 (actually the force is a line force because a situation is considered which is infinite in the y direction). For this case the

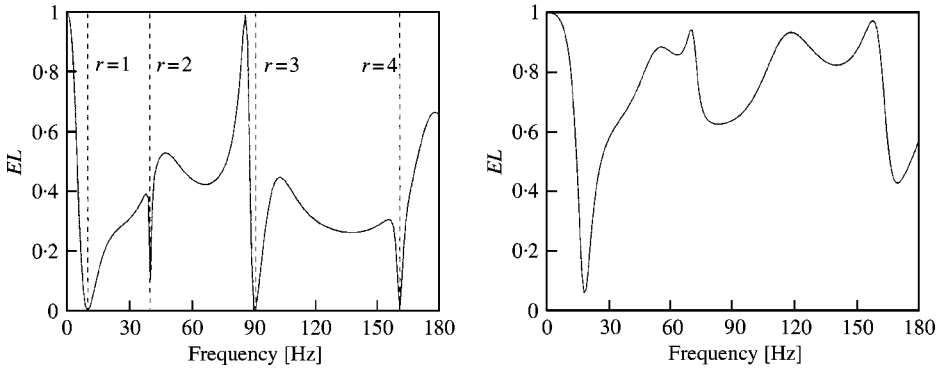

Figure 11. Energy loss for the identical (left) and non-identical (right) double-wall panel, $2h_0 = 1$ mm, excited with the pressure field given in equation (43).

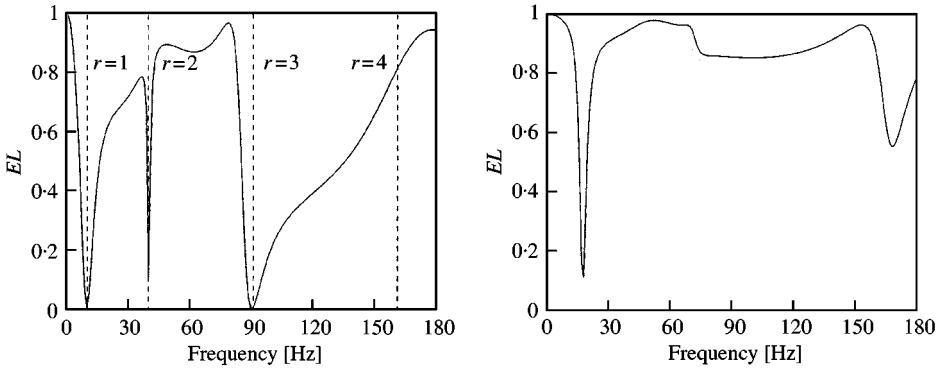

Figure 12. Energy loss for the identical (left) and non-identical (right) double-wall panel with point excitation, $2h_0 = 1$ mm.

power per unit width that is dissipated by the air layer is given by

$$\bar{W}_d = -\frac{D_1 h_0^2 \omega^4}{2c_0^3} F \operatorname{Im}(h^*(x_f)).$$

For the point source the energy loss is calculated for the double-wall panel with identical and non-identical plates. The results are given in Figure 12. In the case of identical plates, again, no energy is dissipated when the in-phase modes are excited. The fourth in-phase mode ($f \approx 161$ Hz) is not excited, because x_f is located in a node of the corresponding mode shape. For the non-identical plates the fraction of incident energy which is dissipated is much higher.

The figures in this section show that a significant amount of energy can be dissipated by viscothermal effects in the air layer. This dissipation is related to the pumping of air in the layer. In order to create a damping effect, the layer thickness and the ratio of plate thicknesses has to be chosen carefully. If the layer thickness is chosen to be very large, the viscothermal effects are very small. If the layer thickness is very small, the coupling between the two plates is very strong. Then, it will be difficult to excite the plates with a relative motion to each other and a small amount of damping effect is created. These considerations show that the layer thickness has to be chosen to be small while the plates are left to vibrate

independently. For a given frequency range and freedom of parameter choice there might be an optimum configuration.

5.3. PLANE WAVE EXCITATION: SOUND TRANSMISSION LOSS

Consider a plane wave $\bar{P}_i(\bar{x}) = \mathrm{Re}(\frac{1}{2}Ce^{-i\omega\bar{x}/c_0 \sin\theta})$ incident on plate 1 making an angle θ with the normal of plate 1 (see Figure 13). The excitation for the first plate is now the so-called blocked pressure field [18]: $f(x) = \mathrm{Re}(c_0^4 C/D_1 h_0 \omega^4 \, e^{-ix\sin\theta})$. In the case of an acoustic excitation it is quite common to consider the sound transmission not in terms of energy loss but in terms of sound transmission loss TL which is calculated from

$$TL = 10 \log (\bar{W}_{in}/\bar{W}_{rad,2}). \tag{49}$$

$\bar{W}_{in}$ is in this case the power per unit width of the incident wave:

$$\bar{W}_{in} = (C^2 l_x \cos\theta/4\rho_0 c_0) + \bar{W}_{rad,2}. \tag{50}$$

Because the exterior field is not included in the equations of motion of the plates it is more realistic to add the radiated power of plate 2 to the incident power in order to obtain proper values for the transmission loss. The sound transmission loss for a number of incident angles for both the identical and non-identical panel system is given in Figure 14. It can be seen that for normal incidence ($\theta = 0$) only the symmetric modes are excited and not the asymmetrical modes.

5.4. DIFFUSE SOUND FIELD: SOUND TRANSMISSION LOSS

A more general situation is when a diffuse sound field excites the first plate. The transmission coefficient ($\tau = \bar{W}_{rad,2}/\bar{W}_{in}$) for a diffuse sound field can be obtained from the transmission coefficient for plane waves [19]:

$$\tau_{diff} = \int_0^{\theta_l} \tau_{plane}(\theta) \sin(2\theta) \, d\theta, \tag{51}$$

where θ_l is the limiting angle above which zero incidence is assumed. Experiments indicate that $\theta_l \approx 78^\circ$ [8]. The sound transmission loss is obtained from the transmission coefficient by the relation $TL = 10\log(1/\tau)$. For the given configuration the transmission loss and the energy loss for a diffuse field is given in Figure 15. The transmission loss for diffuse

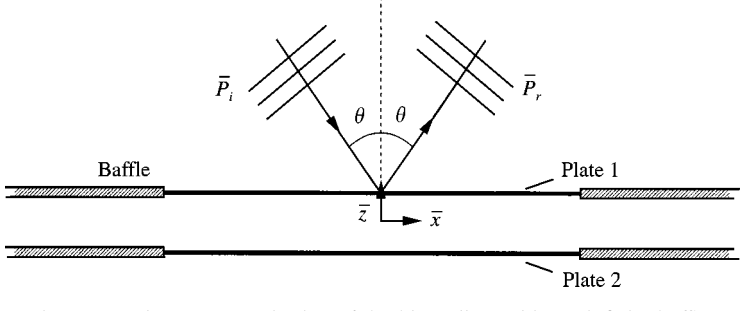

Figure 13. Plane wave excitation of double-wall panel in an infinite baffle.

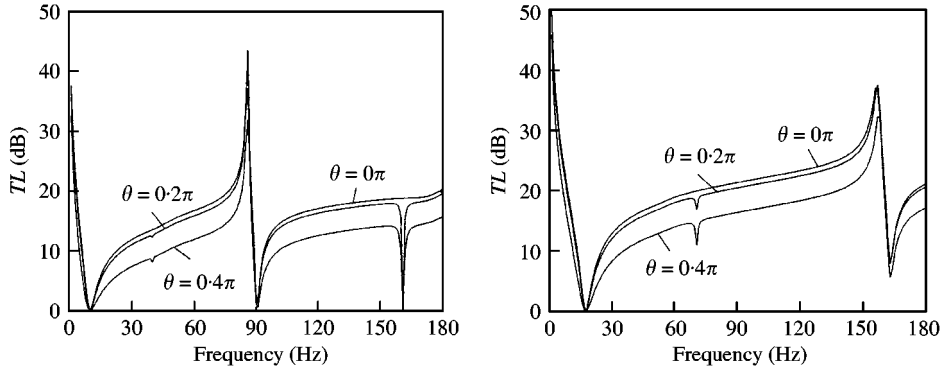

Figure 14. Sound transmission loss for the identical (left) and non-identical (right) double-wall structure for three different angles of incidence, $2h_0 = 1$ mm.

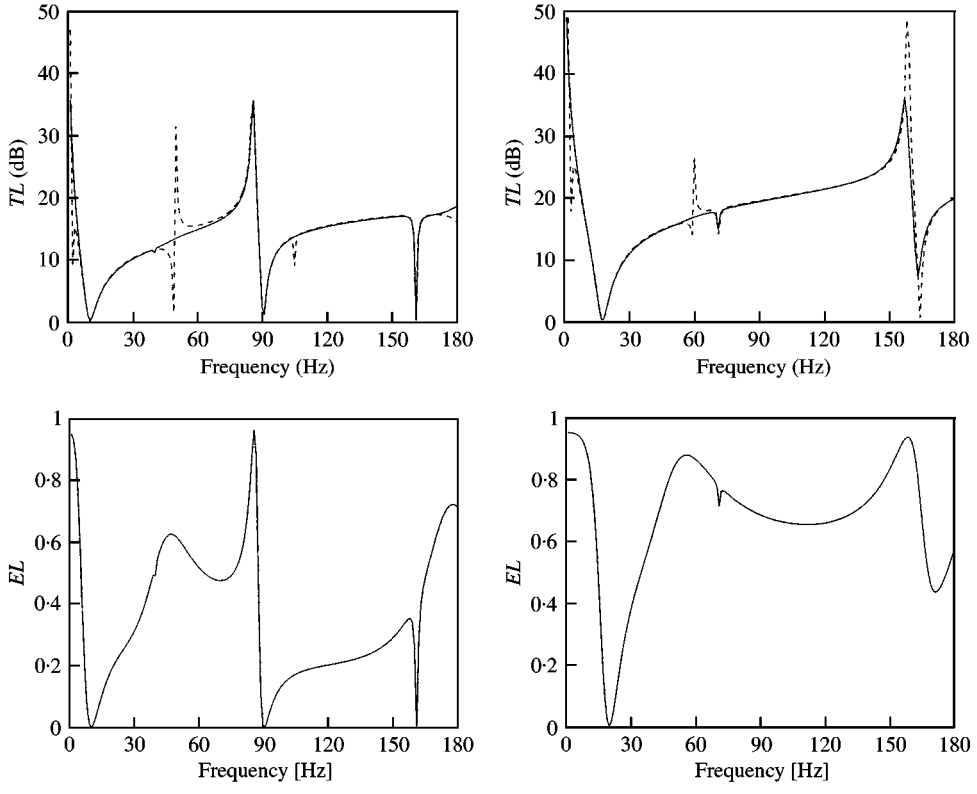

Figure 15. Sound transmission loss and energy loss for the identical (left) and non-identical (right) double-wall structure for a diffuse sound field, $2h_0 = 1$ mm. (——) Viscothermal effects included, (- - - -) adiabatic, inviscid.

sound fields gives results which are somewhere between the results for some single angles of incidence shown in Figure 14. It can be seen as an average of all angles of incidence.

In Figure 15, the transmission loss is also given for the adiabatic and inviscid situation. In this way, the influence of the viscothermal effects becomes visible (note that the energy loss

for the adiabatic and inviscid situation is always zero). Figure 15 shows that the influence of viscothermal effects on the transmission loss is very small. Only around the eigenfrequencies are there small differences between the results. This observation confirms the well-known fact that damping has only effect for resonant behaviour of the panels and hardly influences the overall transmission loss. The transmission loss in the low-frequency region is mainly governed by the mass and stiffness of the panels and there is a minor influence of the damping, an observation which can also be found in standard text books, e.g., reference [18]. It is therefore important to distinguish between the energy loss and the transmission loss. The energy loss is the fraction of incident energy which is dissipated in the air layer, and it is thus a quantity which gives information only about the dissipation. In the transmission loss the power is considered which is travelling towards the panel. This is not necessarily the energy which is injected into the panel because much of the incident energy is reflected. The transmission loss therefore gives information about the combined effect of reflection and dissipation by the panel. Thus, the transmission loss can be high while there is no energy dissipation and the energy loss is low.

6. DISCUSSION AND CONCLUSIONS

A new, very efficient analytical model is used to predict the vibrational and acoustic behaviour of double-wall panels. The model which is used for obtaining the results includes all relevant effects, such as viscothermal wave propagation and full acousto-elastic interaction. Furthermore, the model is, compared with other models including all effects, highly efficient, which makes it possible to perform design studies easily. In this paper, only simply supported double-panel systems, infinite in one direction and with open edges are discussed. It is possible, although not straightforward, to use more complicated configurations and other boundary conditions than discussed in this paper. This will result in slightly more complicated models for which the general conclusions drawn in this paper will also hold. Also fluids other than air and other plate materials can be used. From the results given in this paper it can be concluded that the damping and energy loss can be greatly increased by taking advantage of the dissipative behaviour of small air layers. The damping is mainly introduced by the viscosity of the medium. Thermal effects play a minor role for the damping properties. This was already observed by Fox and Whitton [12]. The influence of viscothermal effects on the transmission loss is limited to small frequency bands around eigenfrequencies of the panel. Furthermore, the solutions presented are suitable as a reference for testing numerical codes.

ACKNOWLEDGMENTS

The authors wish to thank E. Damhof, W. M. Beltman, F. J. M. van der Eerden, M. H. H. Oude Nijhuis and R. Visser for their contribution. This research project is supported by the Dutch Technology Foundation (STW).

REFERENCES

1. W. M. BELTMAN 1998 *Ph.D. Thesis, University of Twente*. Viscothermal wave propagation including acousto-elastic interaction. ISBN 90-365-1217-4.
2. W. M. BELTMAN, P. J. M. VAN DER HOOGT, R. M. E. J. SPIERING and H. TIJDEMAN 1997 *Journal of Sound and Vibration* **206**, 217–241. Air loads on a rigid plate oscillating normal to a fixed surface.

3. W. M. BELTMAN, P. J. M. VAN DER HOOGT, R. M. E. J. SPIERING and H. TIJDEMAN 1998 *Journal of Sound and Vibration* **216**, 159–185. Implementation and experimental validation of a new viscothermal acoustic finite element for acousto-elastic problems.
4. W. M. BELTMAN 1999 *Journal of Sound and Vibration* **227**, 555–586. Viscothermal wave propagation including acousto-elastic interaction. Part I: theory.
5. W. M. BELTMAN 1999 *Journal of Sound and Vibration* **227**, 587–609. Viscothermal wave propagation including acousto-elastic interaction. Part II: applications.
6. L. L. BERANEK and G. A. WORK 1949 *Journal of the Acoustical Society of America* **21**, 419–428. Sound transmission through multiple structures containing flexible blankets.
7. A. LONDON 1950 *Journal of the Acoustical Society of America* **22**, 270–279. Transmission of reverberant sound through double walls.
8. K. A. MULHOLLAND, H. D. PARBROOK and A. CUMMINGS 1967 *Journal of Sound and Vibration* **6**, 324–334. The transmission loss of double panels.
9. A. TROCHIDIS 1982 *Acoustica* **51**, 201–212. Vibration damping due to air or liquid layers.
10. A. TROCHIDIS and A. KALAROUTIS 1986 *Journal of Sound and Vibration* **107**, 321–327. Sound transmission through double partitions with cavity absorption.
11. M. MÖSER 1980 *Acoustica* **46**, 210–217. Damping of structure born sound by the viscosity of a layer between two plates.
12. M. J. H. FOX and P. N. WHITTON 1980 *Journal of Sound and Vibration* **73**, 279–295. The damping of structural vibrations by thin gas films.
13. T. ÖNSAY 1993 *Journal of Sound and Vibration* **163**, 231–259. Effects of layer thickness on the vibration response of a plate-fluid layer system.
14. W. DESMET and P. SAS 1994 in *ISMA* 19 *Conference on Noise and Vibration Engineering*, 101–123, Leuven. Katholieke universiteit, Leuven. The effect of sound absorbing materials, plate stiffeners and vibration isolators on the vibro-acoustic behaviour of finite double wall structures.
15. L. C. CHOW and R. J. PINNINGTON 1987 *Journal of Sound and Vibration* **118**, 123–139. Practical industrial method of increasing structural damping in machinery. I: Squeeze film damping with air.
16. F. DAMHOF 1997 *Master's Thesis, University of Twente, Department of Mechanical Engineering Enschede, The Netherlands.* Acousto-elastic behaviour of double wall structures with viscothermal gaslayers.
17. W. M. BELTMAN, T. G. H. BASTEN and H. TIJDEMAN 1999 in *American Society of Mechanical Engineers International Mechanical Engineering Congress and Exposition* volume MD-Vol. 87, 387–395, Nashville. Viscothermal damping in thin gas or fluid layers.
18. F. J. FAHY 1985 *Sound and Structural Vibration.* New York: Academic Press; first edition.
19. A. D. PIERCE 1981 *Acoustics, an Introduction to its Physical Principles and Applications.* Acoustical Society of America; 1994 edition.

APPENDIX A: COMPUTATION OF THE EIGENFREQUENCIES OF A TWO-DIMENSIONAL DOUBLE-WALL PANEL

In this appendix the solution procedure for deriving the eigenfrequencies of a double-wall panel, infinite in one direction, with simply supported plates and a narrow open air layer in between, is presented. The three equations governing the problem are:

$$\frac{\mathrm{d}^2 p}{\mathrm{d}x^2} = \frac{\gamma}{B(s)}\left[\frac{p}{n(s\sigma)} + \frac{1}{2}(h_1 - h_2)\right], \tag{A.1}$$

$$\frac{\mathrm{d}^4 h_1}{\mathrm{d}x^4} - \frac{\Omega_1^2}{k_{px}^4} h_1 = \frac{\Omega_1^2 \varepsilon_1}{\gamma k_{px}^4 k^2} p, \tag{A.2}$$

$$\frac{\mathrm{d}^4 h_2}{\mathrm{d}x^4} - \frac{\Omega_2^2}{k_{px}^4} h_2 = -\frac{\Omega_2^2 \varepsilon_2}{\gamma k_{px}^4 k^2} p. \tag{A.3}$$

The boundary conditions for simply supported plates and an open air layer are

$$p = 0 \quad \text{for } x = \pm k_{px}, \tag{A.4}$$

$$h_{1,2} = 0 \quad \text{for } x = \pm k_{px}, \tag{A.5}$$

$$\frac{\mathrm{d}^2 h_{1,2}}{\mathrm{d}x^2} = 0 \quad \text{for } x = \pm k_{px}. \tag{A.6}$$

Substitution of the three differential equations leads to the following differential equation in h_2:

$$\left(\frac{\mathrm{d}^4}{\mathrm{d}x^4} - \frac{\Omega_1^2}{k_{px}^4}\right)\left(\frac{\mathrm{d}^4}{\mathrm{d}x^4} - \frac{\Omega_2^2}{k_{px}^4}\right)\left(\frac{\mathrm{d}^2}{\mathrm{d}x^2} - \frac{\gamma}{B(s)n(s\sigma)}\right)h_2 - \frac{1}{2B(s)k_{px}^4 k^2}(\Omega_1^2\varepsilon_1 + \Omega_2^2\varepsilon_2)\frac{\mathrm{d}^4 h_2}{\mathrm{d}x^4} + \frac{\Omega_1^2\Omega_2^2}{2B(s)k_{px}^8 k^2}(\varepsilon_1 + \varepsilon_2)h_2 = 0. \tag{A.7}$$

An eigenfunction which fulfills the boundary conditions is

$$h_2 = B_r \sin\left(\frac{r\pi}{2}\left(\frac{x}{k_{px}} + 1\right)\right). \tag{A.8}$$

Substitution of this function in equation (A.7) and multiplication by k_{px}^8 leads to the following characteristic equation:

$$\left[\left(\frac{r\pi}{2}\right)^4 - \Omega_1^2\right]\left[\left(\frac{r\pi}{2}\right)^4 - \Omega_2^2\right]\left[-\left(\frac{r\pi}{2}\right)^2\frac{1}{k_{px}^2} - \frac{\gamma}{B(s)n(s\sigma)}\right] - \frac{1}{2B(s)k^2}(\Omega_1^2\varepsilon_1 + \Omega_2^2\varepsilon_2)\left(\frac{r\pi}{2}\right)^4 + \frac{\Omega_1^2\Omega_2^2}{2B(s)k^2}(\varepsilon_1 + \varepsilon_2) = 0. \tag{A.9}$$

This is a non-linear equation in ω from which the roots have to be found. It is easy to see that without coupling, i.e., $\varepsilon_1 = 0$ and $\varepsilon_2 = 0$, the eigenfrequencies of the uncoupled systems are found. From the coupled characteristic equation the complex roots are found with a root finding procedure in MATLAB. For the root finding procedure start values have to be defined. As a first guess the eigenfrequencies of the uncoupled system can be taken. For better convergence it is, however, advisable to take the eigenfrequencies of the inviscid, adiabatic system. These, real-valued, eigenfrequencies follow from the following sixth order polynomial:

$$\left[\left(\frac{r\pi}{2}\right)^4 - \Omega_1^2\right]\left[\left(\frac{r\pi}{2}\right)^4 - \Omega_2^2\right]\left[-\left(\frac{r\pi}{2}\right)^2\frac{k^2}{k_{px}^2} + k^2\right] + \frac{1}{2}(\Omega_1^2\varepsilon_1 + \Omega_2^2\varepsilon_2)\left(\frac{r\pi}{2}\right)^4 - \frac{1}{2}\Omega_1^2\Omega_2^2(\varepsilon_1 + \varepsilon_2) = 0. \tag{A.10}$$

APPENDIX B: NOMENCLATURE

A_r, B_r, C_r	dimensionless amplitudes of participating mode r
C	pressure amplitude of plane wave
$B(s)$	function accounting for viscous or thermal effects
C_p	specific heat at constant pressure
C_v	specific heat at constant volume

c_0	undisturbed speed of sound
$D_j = E_j t_j^3/12(1-v_j^2)$	bending stiffness of plate j
E_j	Young's modulus of plate material j
EL	energy loss
$f_{vac,r}$	vacuum frequency of mode r
$f(x)$	amplitude of pressure excitation
$F(x, t)$	pressure excitation
F_r	coefficient
G	integrated force amplitude
$\bar{h} = h_0[2 + [h_1 - h_2]\mathrm{e}^{\mathrm{i}\omega t}]$	layer thickness
h_0	mean half-year thickness
$H(\omega, x_p) = h_2(x_p)/G$	frequency response function
H_0^2	Hankel function of the second kind, order zero
$h_1\mathrm{e}^{\mathrm{i}\omega t}$	dimensionless deflection of plate 1
$h_2\mathrm{e}^{\mathrm{i}\omega t}$	dimensionless deflection of plate 2
$\mathrm{i} = \sqrt{-1}$	imaginary unit
$\bar{I}$	time-averaged normal intensity
J_0	Bessel function of first kind, order zero
$k = \omega h_0/c_0$	reduced frequency
$k_{px} = \omega l_x/c_0$	dimensionless wave number in the x direction
$k_{py} = \omega l_y/c_0$	dimensionless wave number in the y direction
l_x	half-length in the x direction
l_y	half-length in the y direction
$n(s\sigma)$	polytropic coefficient
$\bar{p} = p_0[1 + p\mathrm{e}^{\mathrm{i}\omega t}]$	pressure
p_0	mean pressure
p	dimensionless pressure amplitude
$Q_r(s)$	coefficient
r	mode number
$s = h_0\sqrt{\rho_0\omega/\mu}$	shear wave number
$\bar{T} = T_0[1 + T\mathrm{e}^{\mathrm{i}\omega t}]$	temperature
T_0	mean temperature
T	dimensionless temperature amplitude
t	time
t_j	thickness of plate j
TL	transmission loss
$\bar{\mathbf{v}} = c_0\mathbf{v}\mathrm{e}^{\mathrm{i}\omega t}$	velocity vector
$\mathbf{v}$	dimensionless amplitude of the velocity vector
$\bar{W}_{in}$	incident power per unit width
$\bar{W}_d$	dissipated power per unit width
$\bar{W}_{rad}$	radiated power per unit width
$\bar{x} = c_0 x/\omega$	x-co-ordinate
x	dimensionless x-co-ordinate
x_f	dimensionless x-co-ordinate of point source location
x_p	dimensionless x-co-ordinate of response location
x'	dimensionless x-co-ordinate of receiving point
$\bar{y} = c_0 y/\omega$	y-co-ordinate
y	dimensionless y-co-ordinate
Y_0	Bessel function of second kind, order zero
$\bar{z} = h_0 z$	z-co-ordinate
z	dimensionless z-co-ordinate
$\Gamma(s)$	propagation coefficient
$\gamma = C_p/C_v$	ratio of specific heats
$\varepsilon_j = \rho_0 h_0/\rho_{pj} t_j$	ratio of mass per unit area
θ	angle between incident wave and plate normal
$\eta_{r,1}, \eta_{r,2}$	modal coefficients
λ	thermal conductivity
μ	dynamic viscosity
v	Poisson's ratio of plate material

$\bar{\rho} = \rho_0[1 + \rho e^{i\omega t}]$	density
ρ_0	mean density of air
ρ	dimensionless density amplitude
ρ_{pj}	density of plate material j
$\sigma = \sqrt{\mu C_p/\lambda}$	square root of the Prandtl number
Ω_j	dimensionless frequency corresponding with plate j
ω	angular frequency
ω_r	eigenfrequency of mode r
τ	transmission coefficient
τ_{plane}	transmission coefficient for plane wave
τ_{diff}	transmission coefficient for diffuse sound field
∇^2	dimensionless differential operator
∇^4	dimensionless differential operator
ζ_r	viscous damping coefficient of mode r
$*$	complex conjugate